CHAPTER IV
RESULTS AND DISCUSSION

This chapter mainly discusses about the ability in cracking and desulfurization of all catalysts for waste tire pyrolysis. The cracking and hydrogenation abilities of Rh-promoted catalysts was explained in terms of the effects of Rh supported different zeolites (KL, HY and HBETA) with the difference in acidity, pore size, Si/Al ratio and their structures (straight and zig-zag pore). Moreover, two commercial dehydrosulfurization catalysts were also investigated for their cracking activity as well as desulfuring ability. The oils obtained from both the commercial sulfided metal and Rh-promoted catalysts were analyzed for sulfur-containing molecules. The sulfur removal ability was proven by the distribution of sulfur in pyrolysis products.

4.1 Rh-promoted catalysts

The different zeolites (KL, HY and HBETA) were used as a support for Rh. The catalysts were prepared by incipient wetness impregnation technique. The effects of the catalysts on pyrolysis products are elucidated below.

4.1.1 Comparison between acid and basic supports

In order to eliminate the influence of zeolite pore structure, KL and HBETA zeolites were selected to investigate the acidity effect since KL and HBETA zeolites also had straight pore channels with intersecting straight 12-ring channels.

4.1.1.1 Pyrolysis yields

The product distributions of the non-catalytic case, Rh/KL, and Rh/ HBETA catalysts are shown in Figure 4.1. The results show that the catalytic cases give a lower amount of liquid product than the non-catalytic case. It means that using the catalyst can decrease the yield of oil or liquid products along with an increase in the yield of gaseous products as compared to the non-catalytic case. A high gas yield is observed in the set of HBETA cases, and obviously reaches the highest in the case of 0.25 % Rh/HBETA. HBETA (acidic zeolite) leads to

deeper cracking of large molecules to gaseous products than KL (non-acidic zeolite). Another reason was on the larger pore opening of HBETA (7.6 x 6.4 A^{o} in a diameter) that allows bulky molecules to enter to be cracked inside its pore more easily (as compared to 7.1 A^{o} of KL). Moreover, the liquid fraction tends to decrease even by as small amount as 0.25 wt% of Rh loading on HBETA; however, 1 % Rh loading gives a lower gas formation, indicating a lower cracking performance of the catalyst. The results can be explained that the catalysts used in waste tire pyrolysis have different unique properties. However, the yield of solid product is quite similar, that is around 39 wt% in all runs due to the fact that all pyrolysis conditions are kept constant and the tire is same completely decomposed to charcoal product at 500 ^{o}C.

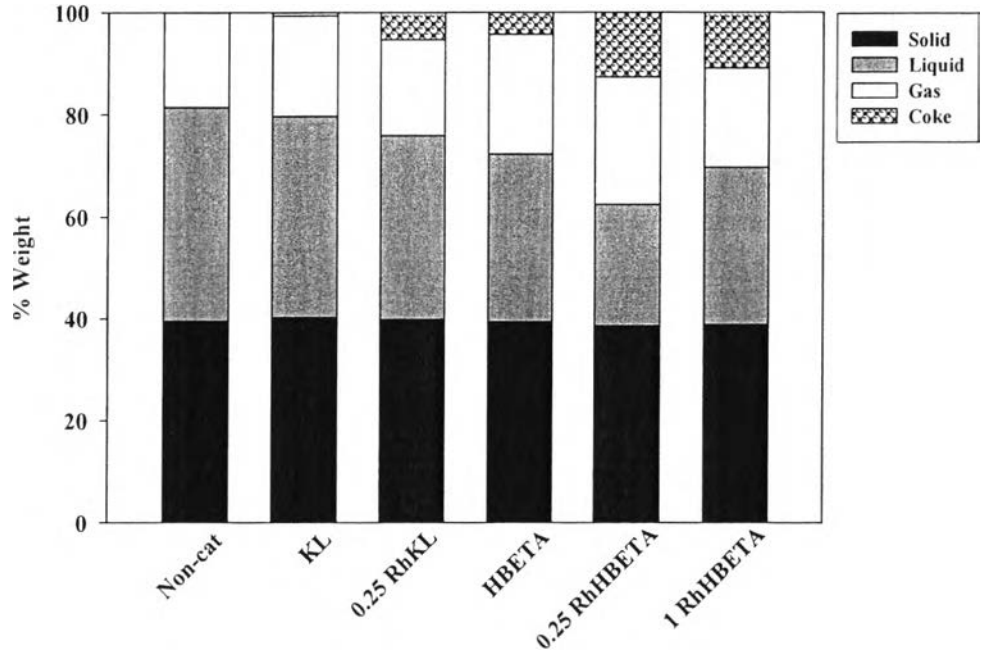

Figure 4.1 Product distribution obtained from the non-catalytic pyrolysis, Rh-promoted KL, and Rh-promoted HBETA catalysts.

Besides gas, liquid and solid products, coke also occurs during pyrolysis process. It is undesired product that deposits on the catalysts and poisons the active size, resulting in catalyst deactivation; so, the involved reactions cannot further take place. Table 4.1 shows the amount of coke (g/g cat) obtained from TG/DTA. The results indicate that HBETA gives twice as much as coke deposited on KL, possibly due to its acidity that causes more coke formation. Furthermore, the larger pore opening of HBETA seen in Table 4.1 induces the formation of big hydrocarbon molecule (Dũng *et al.*, 2009). However, the introduction of Rh leads to the decrease in the specific surface area and specific pore volume of catalysts, but increases in the coke formation. The highest coke formation is found in the run of 0.25 wt% Rh/HBETA

Table 4.1 Physical properties of the Rh-promoted KL and HBETA catalysts and the amount of coke in the used catalysts

Sample	Specific surface area (m^2/g)	Pore specific volume (cm^3/g)	Median pore width (Å)	Coke (g/g cat)
KL	239.9	0.267	6.677	0.149
0.25RhKL	209.3	0.190	7.219	0.197
HBETA	525.7	1.012	8.040	0.272
0.25RhHB	518.1	0.565	7.969	0.345
1RhHB	500.1	0.931	7.705	0.301

4.1.1.2 Gas composition

Light olefins obtained from waste tire pyrolysis are highly composed of ethylene and propylene, which are very valuable for petrochemical industry. Figure 4.2 represents the difference of light olefins yields observed from all cases. The results indicate that the highest yield of total light olefins is found in the non-catalytic case, then followed by the sets of KL and HBETA supports, respectively. Hence, KL seems to be the better support for light olefins production than HBETA. Besides, the presence of small Rh loading results in an insignificant increase of ethylene.

On the other hand, the catalytic ability of these catalysts in cooking gas production is opposite to that in light olefins formation. The cooking gas is hereby identified as the combination of propane and mixed-C_4 as shown in Figure 4.3. The series of HBETA leads to a considerable mixed-C_4 formation that results in the highest cooking gas production since no significant difference in propane production is observed. Moreover, the quantities of cooking gas obtained from non-catalytic case and the set of KL are quite similar. However, using the small loading amount of Rh on KL does not affect to propane and mixed-C_4 fractions as compared to on pure KL.

The distribution of all gas components; namely, methane, ethylene, ethane, propylene, propane, mixed-C_4 and C_5, is shown in Appendix C1. It can be observed that using HBETA results in a bit lower C_5 than using KL. The presence of 0.25 wt% of Rh leads to a high selectivity to hydrogenated products in accordance with the reduction of C_5 to the lighter molecule that is apparently due to the fact that noble metal can promote hydrogenolysis reaction.

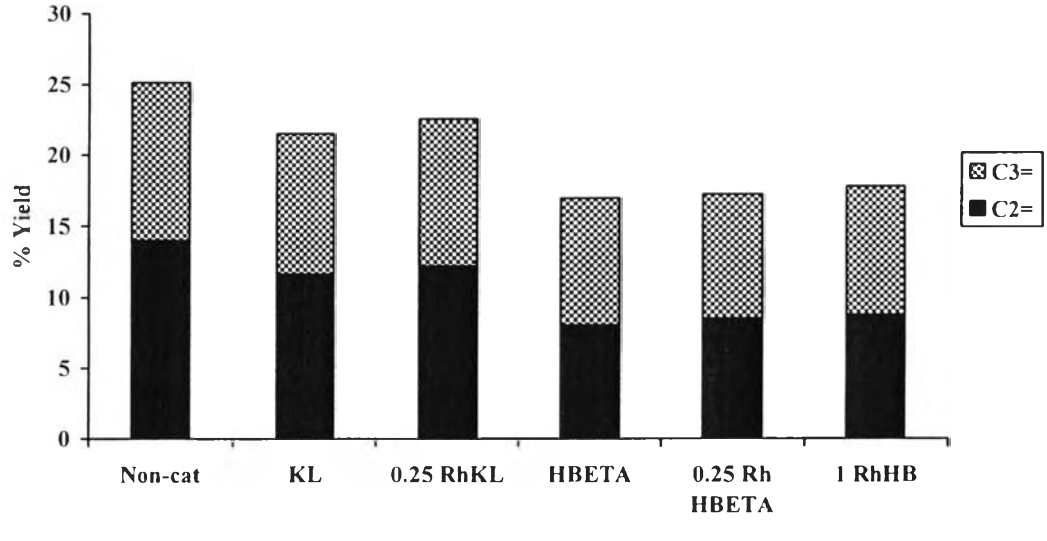

Figure 4.2 Yield of light olefins production obtained from the non-catalytic pyrolysis, and Rh-promoted KL and HBETA catalysts.

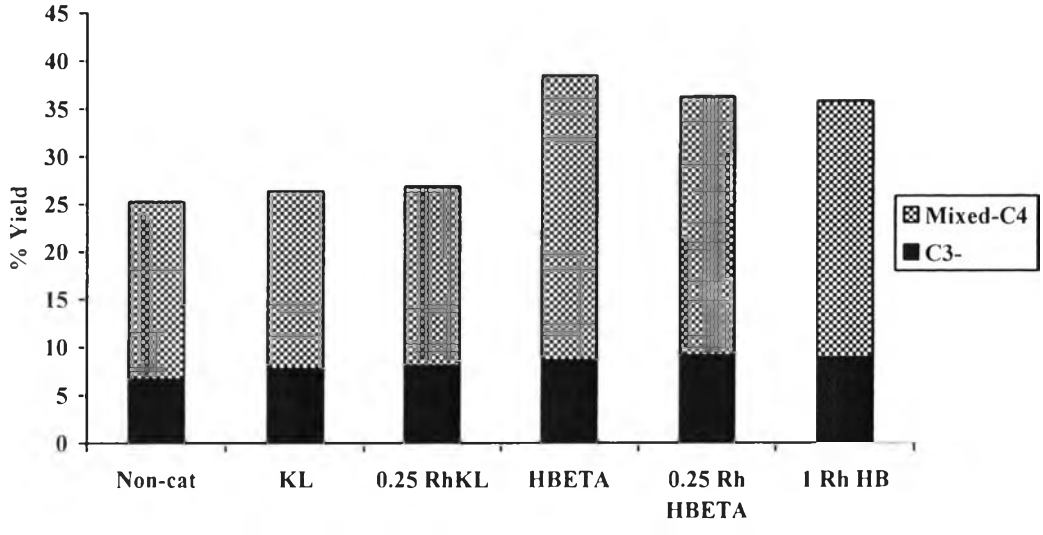

Figure 4.3 Yield of cooking gas production obtained from the non-catalytic pyrolysis, and Rh-promoted KL and HBETA catalysts.

4.1.1.3 Liquid composition and petroleum cuts

The maltenes obtained from waste tire pyrolysis were analyzed by using a SIMDIST Gas Chromatography (SIMDIST-GC): then, the true boiling point curves (TBPs) cut into petroleum fractions according to the boiling point ranges of hydrocarbons, which are full range naphtha (<200 °C), kerosene (200–250 °C), light gas oil (250–300 °C), heavy gas oil (300–370 °C), and long residue (>370 °C) (Dũng *et al.*, 2010) as shown in Appendix D2. It is observed that the oils from all cases contain approximately 40% full range naphtha as the majority. In addition about 20 %, kerosene is found, whereas the light and heavy gas oils and long residue are produced in an approximately equal amount that is around 10 wt%. HBETA has a good cracking activity because it can reduce heavy fractions, i.e. residues and heavy gas oil, better than KL due to the fact that the long-chain hydrocarbons are easily cracked to short-chain hydrocarbons by the acidity of HBETA. The introduction of 0.25 wt% of Rh loading on KL and HBETA gives an increase in full range naphtha as compared to using pure zeolite, possibly because of hydrogenation ability of the noble. However, the cooperation of Rh makes the acidity of zeolite supports decrease, resulting in a lower cracking ability. Moreover, it is

found that the presence of Rh apparently results in mono-aromatics formation as shown in Figure 4.4, and the mono-aromatics outstandingly present in the mono-aromatics fractions of maltenes when Rh is involved in the reaction are quantitatively reported in Table 4.2. The increase of mono-aromatics in maltenes indicates higher value products of mono-aromatics derivatives.

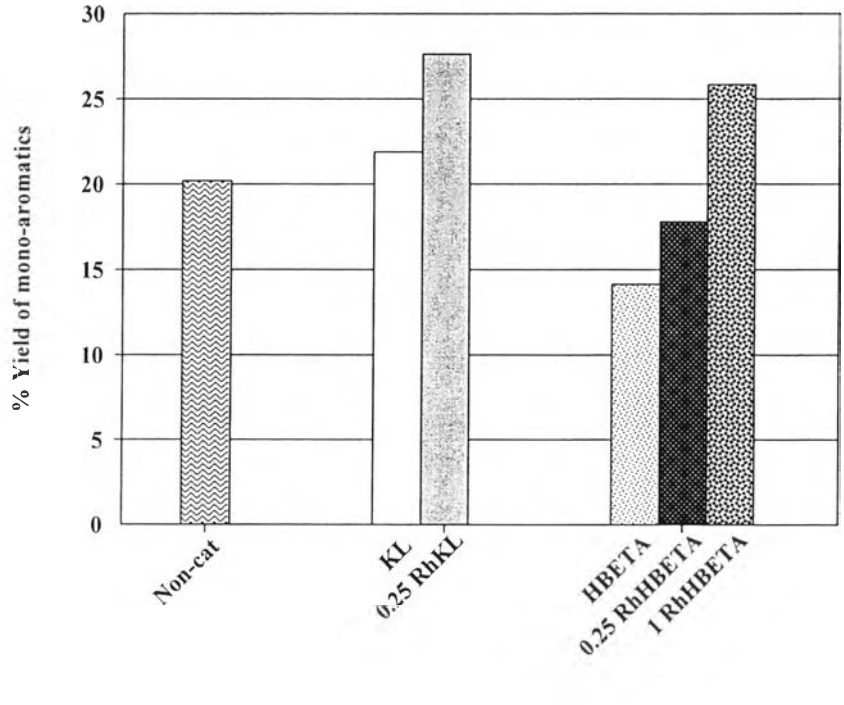

Figure 4.4 Yield of momo-aromatics obtained from non-catalytic pyrolysis, and Rh-promoted KL and HBETA catalysts.

Table 4.2 Prominent mono-aromatics species in mono-aromatics fractions of pyrolysis oils obtained from using Rh supported on KL and HBETA as a catalyst

Name	Area (%)		
	0.25RhKL	**0.25RhHB**	**1RhHB**
Benzene, 1-methyl-2-(1-methylethyl)-	2.111	0.095	1.651
Benzene, 1-methyl-3-(1-methylethyl)-	0.330	1.522	0.277
Benzene, 1-methyl-3-(1-methyl-2-propenyl)-	0.859	0.184	1.410
Benzene, 1-butynyl-	1.950	-	2.188
Benzene, (2-cyclopropylethenyl)-	1.646	-	-
Benzocycloheptatriene	-	3.827	-
Bicyclo[4.2.0]octa-1,3,5-triene, 7-isopropyl-	0.403	1.137	0.157
Ethylbenzene	2.046	1.049	1.101
Styrene	1.571	0.508	0.950
m-Xylene	1.558	0.748	1.174
Naphthalene, 1,2-dihydro-	1.091	0.033	1.403
1H-Indene, 1-ethylidene-	1.254	2.106	3.032
1H-Indene, 2,3-dihydro-4-methyl-	-	1.482	-

4.1.1.4 Sulfur removal activity

The amount of sulfur in pyrolysis oils is determined using a sulfur elemental analyzer (LECO® Elemental Analyzer, CHNS-932). Figure 4.5 exhibits the weight percentage of sulfur in pyrolysis oils from the non-catalytic case, and Rh-promoted KL and HBETA catalysts. The highest sulfur content is found in the non-catalytic case, but it can be alleviated by using the catalysts and KL gives the higher total sulfur content in the pyrolysis oil than HBETA. However, KL gives the contrary result on the amount of polar-aromatics, as seen in Appendix D1, which shows that KL produces a lower amount of polar-aromatics than HBETA. It presumably means that most of sulfur species prefers to be in the forms of other compounds rather than aromatics (such as straight chain) with using KL. The

reduction of polar-aromatics occurs when 0.25 wt% of Rh loading on the HBETA support possibly because the hydrogenation by the noble metal could saturate the aromatics and double bonds before the aromatic rings are open and then cracked, releasing sulfur in the form of hydrogen sulfide. The sulfur content obtained from 1 wt% of Rh loading was similar to 0.25 wt% loading. Figure 4.6 can support that 0.25 % Rh/HBETA well shifts the sulfur-containing molecules in the char and the liquid product to the gas fraction, possibly in the form of hydrogen sulfide (Lin *et al.*, 1997).

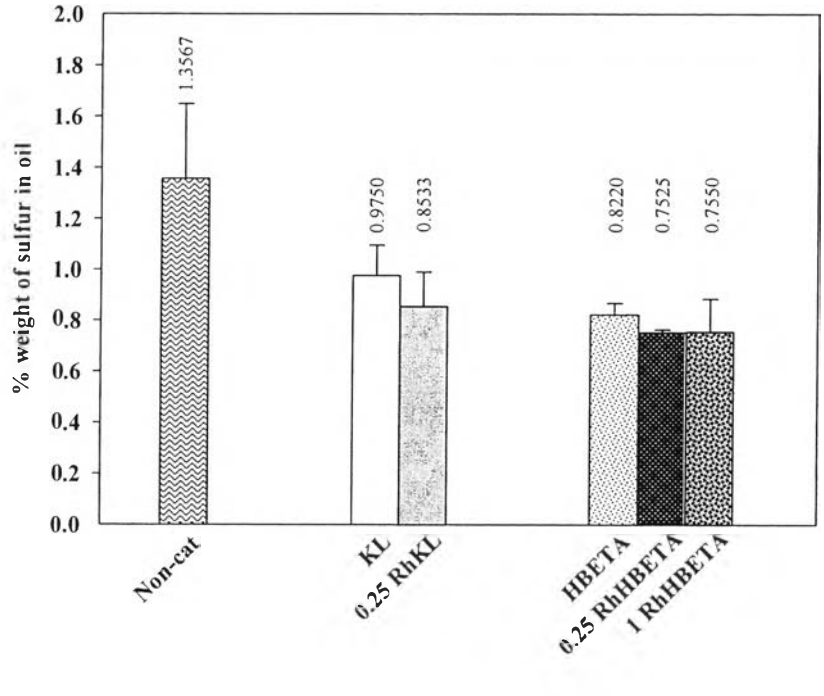

Figure 4.5 % weight of sulfur content in pyrolysis oils obtained from using Rh supported on KL and HBETA.

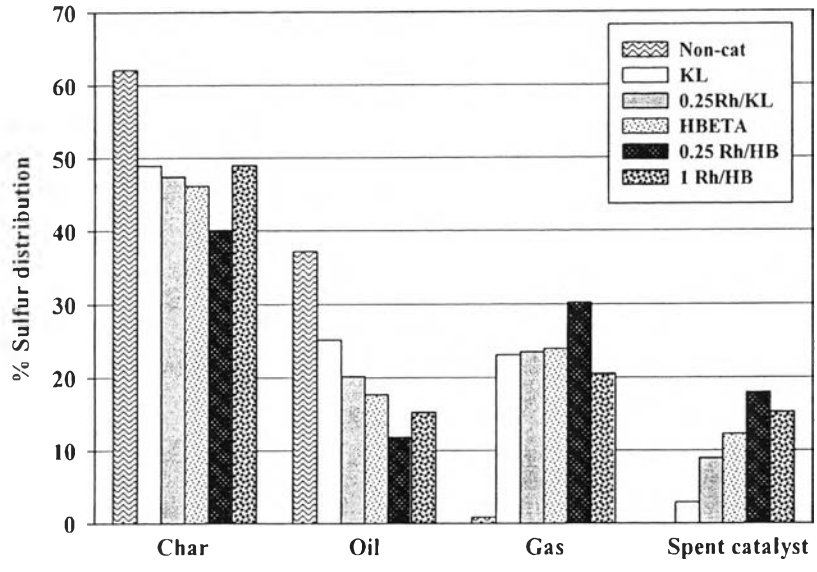

Figure 4.6 Sulfur distribution in pyrolysis products obtained from Rh-promoted KL and HBETA catalysts.

The pyrolysis oils were analyzed by GC-MS (TOF) Mass Analyzer to determine the sulfur species in the liquid products. The sulfur-containing molecules comprised of carbon, hydrogen and sulfur element are found in range of C_3-C_{18}, which is the ranges of gasoline to gas oil determined by the carbon number of C_5-C_9 for gasoline, C_{10}-C_{13} for kerosene and C_{14}-C_{20} for gas oil. Figure 4.7 shows the distribution of sulfur-containing molecules in petroleum fractions. The non-catalytic pyrolysis gives the sulfur-containing compounds highest distributed in the gas oil range and the lowest in the gasoline range. The introduction of the catalysts changes the distribution of sulfur-containing compounds to a range of lighter fractions. The sulfur compounds in the case of HBETA are highly distributed in kerosene. Moreover, the presence of Rh shifts the distribution of sulfur compounds into the gasoline range. It shows that the catalysts have the ability in both cracking and desulfurization.

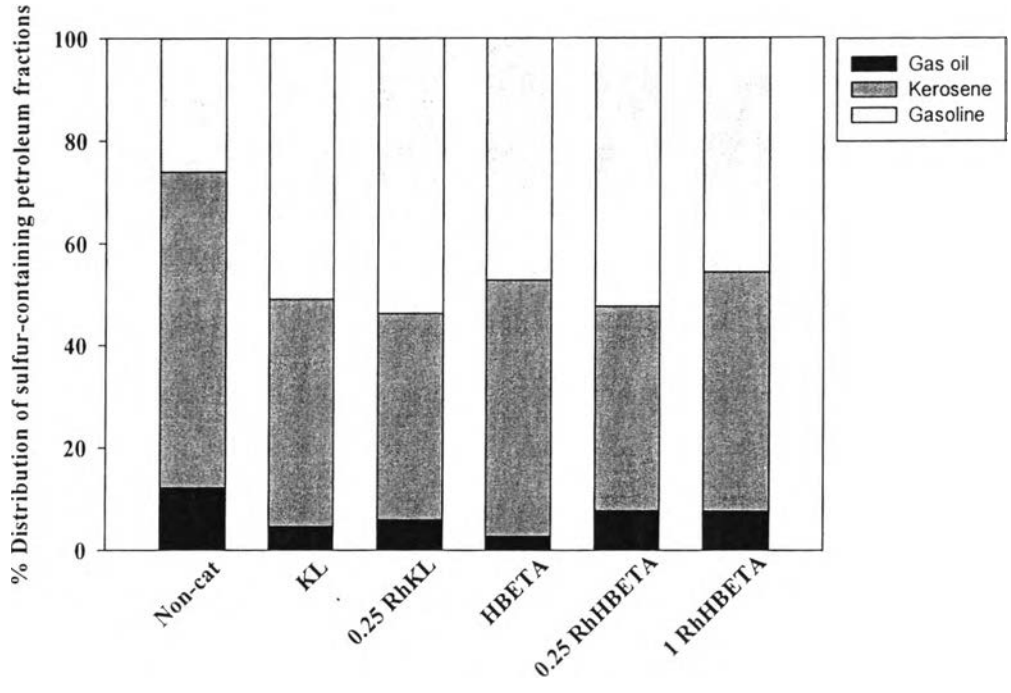

Figure 4.7 Distribution of sulfur-containing compounds in petroleum fractions.

Appendices G1-G10 show the sulfur species found in pyrolysis oils by using a GC-TOFMS Mass Analyzer. The top five species of the sulfur-containing molecules mostly present in the pyrolysis oils are benzothiophene derivatives as follows: 3-methylbenzothiophene (C_9H_8S), benzo[b]thiophene, 2,5-dimethyl- and 2,7-dimethyl- ($C_{10}H_{10}S$), benzo[b]thiophene, 2-ethyl-7-methyl- and 2,5,7-trimethyl- ($C_{11}H_{12}S$) as shown as the examples in Figure 4.8. Unlike these results, Williams and Bottrill (1995) found mainly dibenzothiophene derivatives containing rich of trimethyl-dibenzothiophene, indicating that the obtained oils had higher quality than those from their work because the sterically-hindered sulfur compounds are diminished due to deep hydrodesulfurization (Tang and Shi, 2011). The prominent C, H, S-containing molecules found in pyrolysis oils are reported in Table 4.3. It is observed that the catalytic pyrolysis using Rh/HBETA catalysts mostly causes the formation of dimethyl-benzothiophenes.

Table 4.3 Prominent C, H, S-containing molecules found in pyrolysis oils from Rh-promoted KL and HBETA catalysts

Name	Area (%)					
	Non-catalyst	Non-acidic catalyst		Acidic catalyst		
		KL	0.25Rh KL	HB	0.25Rh HB	1Rh HB
T, 2-(1-methylethyl)-	0.0117	0.0182	0.003	0.0493	0.0314	0.0189
BT	0.0283	0.0551	0.0539	0.0432	0.0911	0.0888
BT, 2-methyl-	0.0187	0.0719	0.0602	0.0589	0.0005	0.001
BT, 6-methyl-	-	0.0414	-	0.0442	0.0457	0.0458
3-Methyl Benzothiophene	0.0499	0.0307	0.0618	0.0247	0.1361*	0.1614*
BT, 2,5-dimethyl-	0.0409	0.1189*	0.0193	0.1068*	0.0249	0.0487
BT, 2,7-dimethyl-	0.1138*	0.0401	0.1019*	0.0316	0.0939	0.1665*
BT, 2-ethyl-7-methyl-	0.0606	0.026	0.0022	0.0425	0.1001*	0.0025
BT, 2,5,7-trimethyl-	0.0446	0.0034	0.003	0.0029	0.0056	0.1379*
BT, 7-ethyl-2-methyl-	0.0077	0.0022	0.0637	0.0298	0.0046	0.0055
BT, 2,7-diethyl-	0.0463	0.0305	0.001	0.0556	0.0033	0.0042

T = Thiophene

BT = Benzo[b]thiophene

* The area percentage of C,H,S-containing molecules in maltene fraction greater than 0.1 %

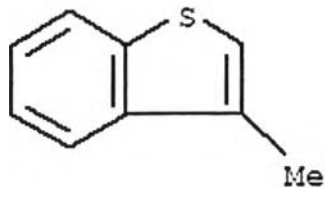

3-Methylbenzothiophene

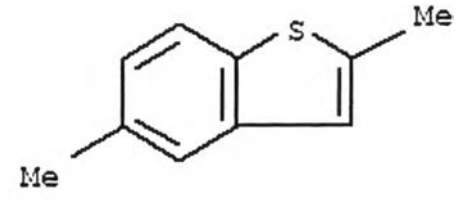

Benzo[b]thiophene, 2,5-dimethyl-

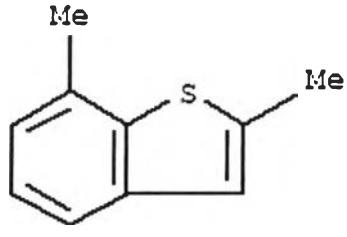

Benzo[b]thiophene, 2,7-dimethyl-

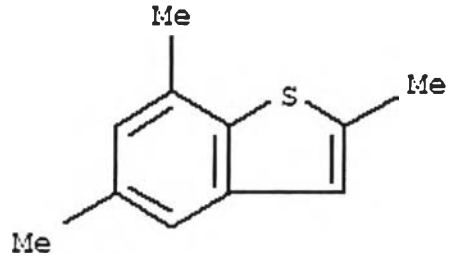

Benzo[b]thiophene, 2,5,7-trimethyl

Figure 4.8 Examples of sulfur-containing compounds found in pyrolysis oils.

4.1.2 Effect of pore structure

HY and HBETA have a large and indifferent pore opening (0.74 A^o and 7.6 x 6.4 A^o of HY and HBETA, respectively). Both are acidic zeolites, but their structures are different (straight and zig-zag pore) with the Si/Al ratios of 7.5 (HY) and 13.5 (HBETA). Certainly, the quality and quantity of pyrolysis products obtained from the zig-zag pore of HY may differ from those produced by the straight pore of HBETA. Therefore, HY and HBETA were selected as the supports in order to investigate the effects of Si/Al ratio and pore structures.

4.1.2.1 Pyrolysis yields

Figure 4.9 displays the product distribution obtained from the Rh-promoted HY and HBETA catalysts. It can be observed that the liquid product can be diminished in conjunction with the evolutions of gas and coke by using the catalysts. HY gives a bit lower liquid product than HBETA by forming the coke deposited on the spent catalyst. The introduction of 0.25 wt% Rh on HY causes the lower performance of catalyst whereas loading Rh on HBETA deeply promotes the cracking ability. 0.25 wt% Rh/HBETA gives the lowest liquid yield with providing higher gaseous yield as illustrated in Figure 4.9; however, it also induces the highest coke formation.

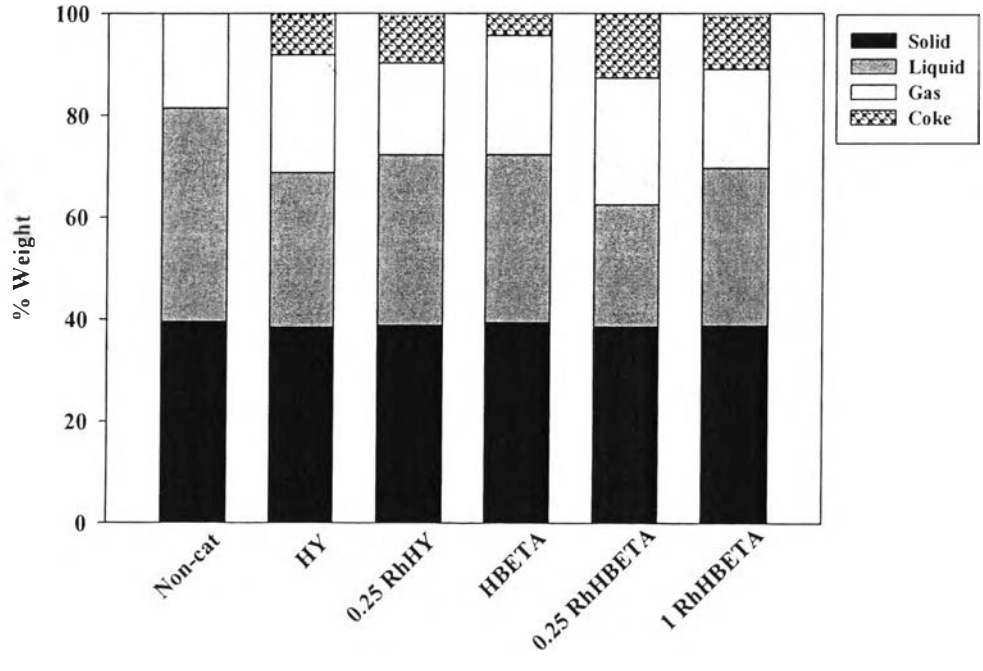

Figure 4.9 Product distribution obtained from the Rh-promoted HY and HBETA catalysts.

The amounts of coke (g/g cat) determined from TG/DTA are shown in Table 4.4. The results indicate that both acidic catalysts give the same amount of coke of around 0.27 g/g catalyst, possibly due to their large pore size. The introduction of Rh brings about the reduction of specific surface area and pore volume, but it increases in the coke formation on HBETA better than HY. The one reason is that the higher acid strength of HBETA may allow more formation of coke molecules to occur on the surface whereas HY has lower acid strength; therefore, large molecules of coke can be formed less easily.

Table 4.4 Physical properties of the Rh-promoted HY and HBETA catalysts and the amount of coke in the used catalysts

Sample	Specific surface area (m^2/g)	Pore specific volume (cm^3/g)	Median pore width (Å)	Coke (g/g cat)
HY	547.7	0.438	7.788	0.270
0.25RhHY	531.1	0.415	7.927	0.274
HBETA	525.7	1.012	8.040	0.272
0.25RhHB	518.1	0.565	7.969	0.345
1RhHB	500.1	0.931	7.705	0.301

4.1.2.2 Gas composition

Figure 4.10 presents the difference in light olefins yield. The results show that the maximum yield of total light olefins is found in the non-catalytic case, then followed by the sets of HY and HBETA supports, respectively. HY shows a higher selectivity for light olefins production than HBETA.

On the contrary, the catalytic activity of these catalysts in terms of cooking gas production is opposite to that of light olefins formation as compared in Figures 4.10 and 4.11. The prominent yield of cooking gas obtained from using HBETA as a support indicates that HBETA has the higher selectivity for cooking gas production, especially mixed-C4 formation. Loading 0.25 wt% of Rh does not promote the activity for light olefins and cooking gas productions of the HY catalyst. However, the amount of propane is not different with using the same support.

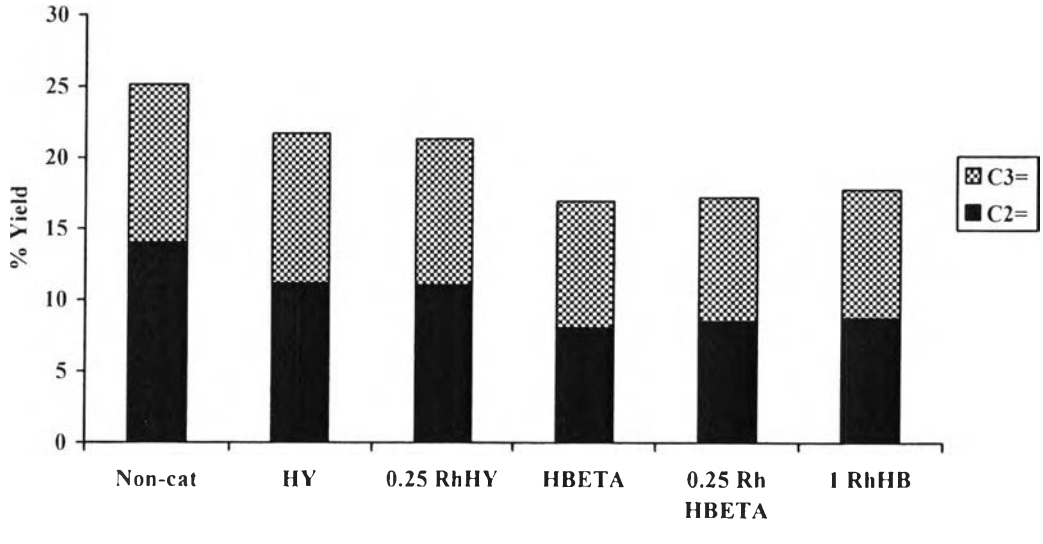

Figure 4.10 Yield of light olefins production obtained from Rh-promoted HY and HBETA catalysts.

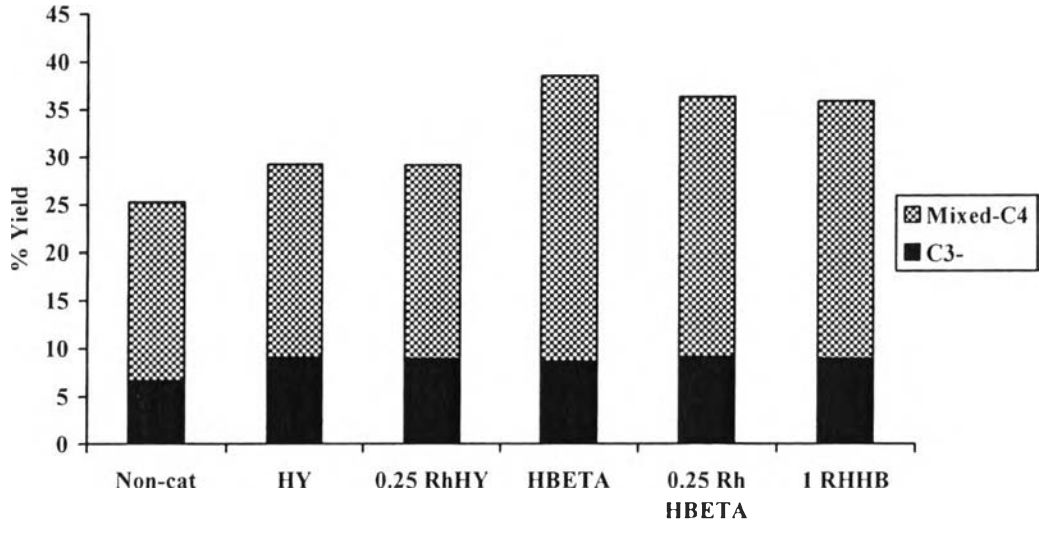

Figure 4.11 Yield of cooking gas production obtained from Rh-promoted HY and HBETA catalysts.

4.1.2.3 Liquid composition and petroleum cuts

The yields of petroleum fractions of derived oils from Rh-promoted HY and HBETA catalysts are shown in Figure 4.12. HBETA has a higher activity for the reduction of heavy fractions, i.e. residues and heavy gas oil than HY, resulting in the production of full range naphtha. Although HY has a lower cracking ability than HBETA, it gives a higher amount of full range naphtha than using HBETA. Therefore, both HY and HBETA influence the quantity of pyrolysis oil because of its acidity. According to the high activity of HBETA support and its straight pore, Rh loading on HBETA causes higher activity, resulting in higher coke formation that would prevent the large molecules to enter to its pore; so, the poly-aromatics remain in the oils as seen in Appendix D1. Appendix D2 shows that the highest cracking extent of long residue is found in the case of HBETA. The Rh loading on HY does not help the cracking reaction while Rh loading on HBETA does. It can be explained by using the results from IPA-TPD analysis (Kresnawahjuesa *et al.*, 2000 and Farneth and Gorte, 1995). TPD profiles in Figure 4.13 present the MS signals of isopropylamine (m/e = 44), ammonia (m/e =17) and propylene (m/e = 41) from a mass spectrometer. The maximum desorption of

unreacted isopropylamine on the HBETA supports are observed at 102 °C, associating to weak acid sites on the surface of HBETA while HY samples show no peak of unreacted isopropylamine, meaning that HBETA has more amount of weak acid sites as seen in Figure 4.13(a). The peaks of propylene and ammonia in Figure 4.13(b) and 4.13(c) represent Brønsted acid sites that appear at a higher temperature after the decomposition of isopropylamine to propylene and ammonia occurs on this site. It is clearly seen that HY hardly has the Brønsted acid sites, especially the 0.25Rh/HY sample. Moreover, the Brønsted acid strength of pure HBETA seems to be higher than loading Rh on HBETA as observed by the higher desorption temperature of ammonia. It is observed that the introduction of Rh slightly decreases the acidity of the catalyst, resulting in a lower ability on the cracking of long residue fraction.

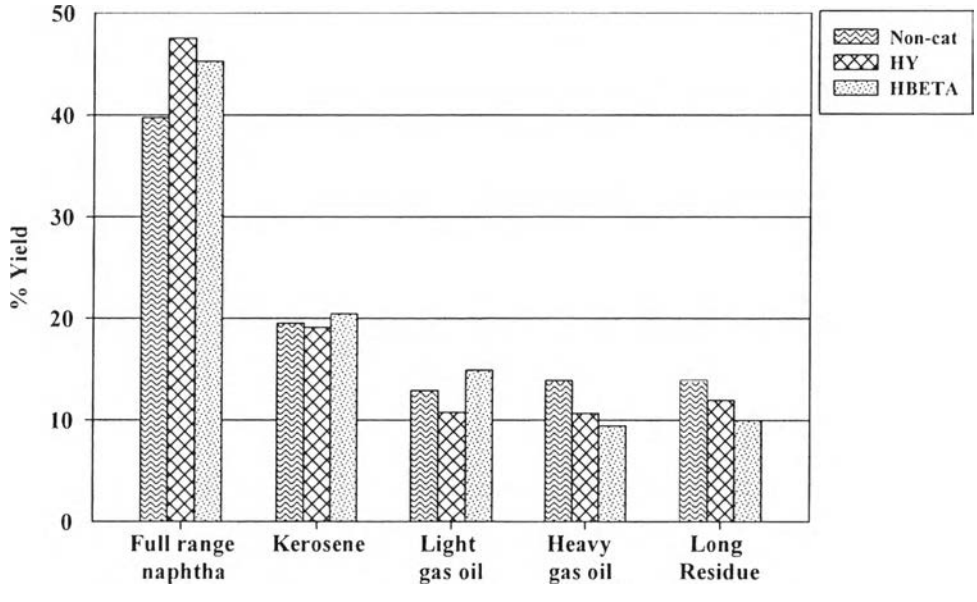

Figure 4.12 Yield of petroleum fractions in derived oils from the non-catalytic pyrolysis, pure HY, and pure HBETA.

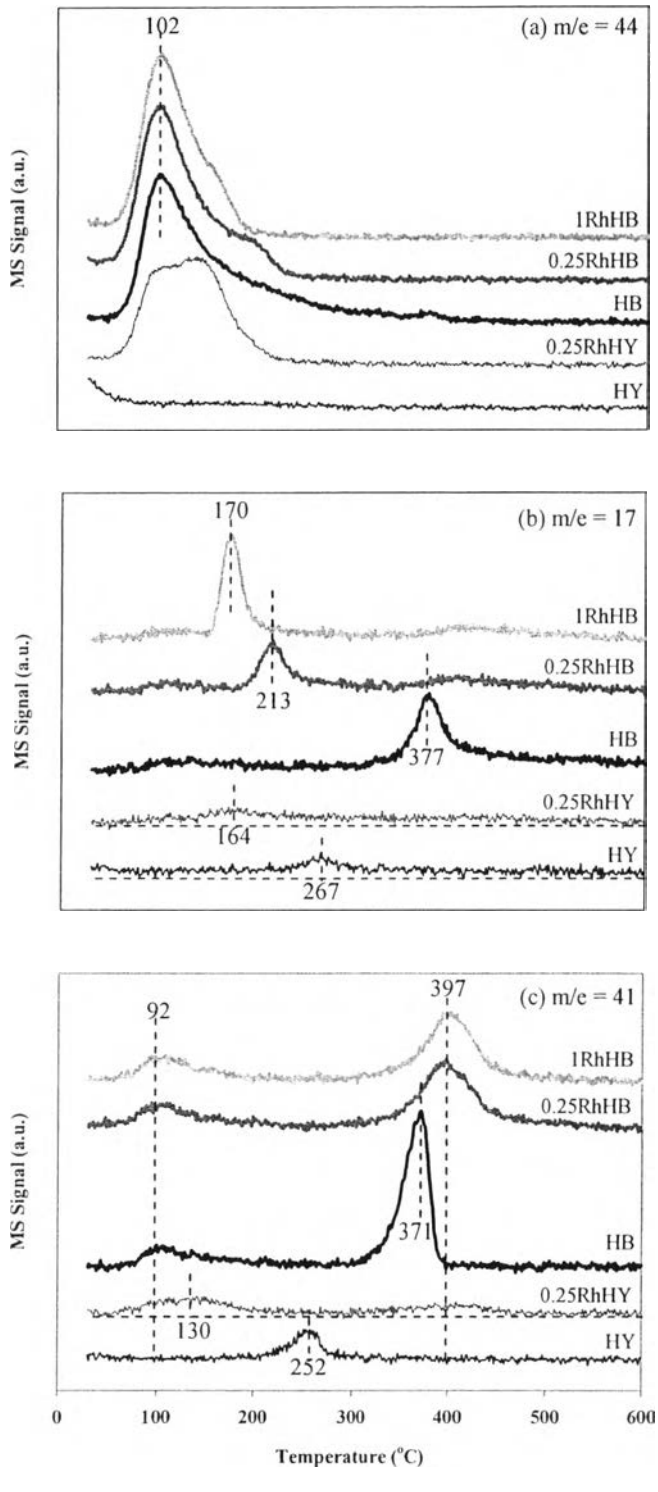

Figure 4.13 IPA-TPD profiles of (a) isopropylamine desorption, (b) ammonia formation, and (c) propylene formation on Rh-promoted HY and HBETA catalysts.

The remarkable production of mono-aromatics is observed since Rh metal participates in the reaction as shown in Figure 4.14, and the prominent mono-aromatics molecules in the pyrolysis oils obtained from using Rh supported on HY and HBETA as a catalyst are reported in Table 4.5. 0.25 % Rh/HY, 0.25 % Rh/HBETA and 1 % Rh/HBETA give a high selectivity in benzene, 1-methyl-2-(1-methylethyl)-, benzocycloheptatriene, and 1H-Indene, 1-ethylidene-, respectively.

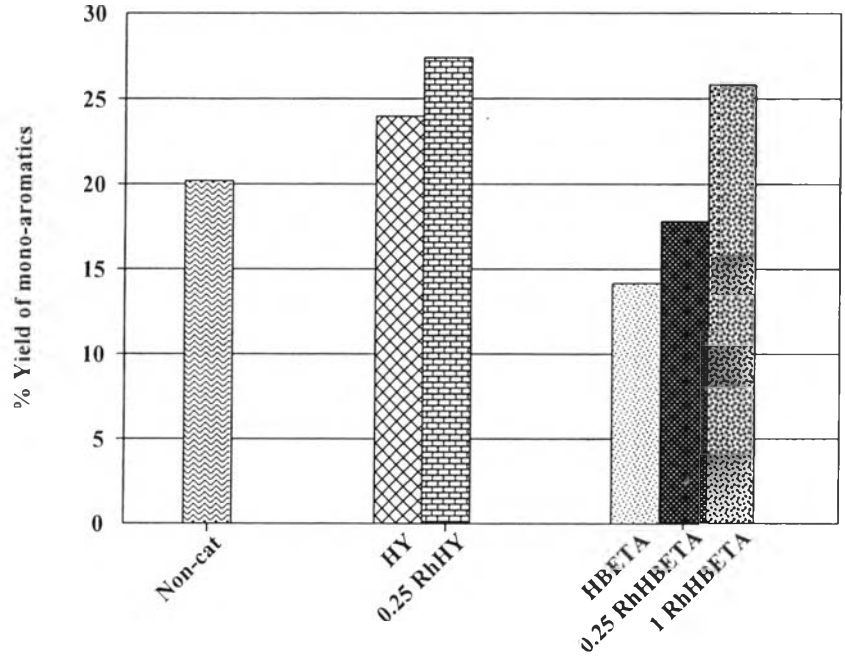

Figure 4.14 Yield of momo-aromatics obtained from the non-catalytic pyrolysis, and the sets of Rh-promoted HY and HBETA catalysts.

Table 4.5 Prominent mono-aromatics molecules in pyrolysis oils obtained from using Rh supported on HY and HBETA as a catalyst

Name	Area (%)		
	0.25RhHY	**0.25RhHB**	**1RhHB**
Benzene, 1-methyl-2-(1-methylethyl)-	2.9286	0.0949	1.6508
Benzene, 1-methyl-3-(1-methylethyl)-	0.3261	1.5219	0.2774
Benzene, 1-methyl-3-(1-methyl-2-propenyl)-	-	0.1835	1.4096
Benzene, 1-butynyl-	1.3074	-	2.1876
Benzene, (2-cyclopropylethenyl)-	0.5205	-	-
Benzocycloheptatriene	-	3.8273	-
Bicyclo[4.2.0]octa-1,3,5-triene, 7-isopropyl-	1.1504	1.1372	0.1567
Ethylbenzene	1.9314	1.0494	1.1010
Styrene	1.0625	0.5080	0.9502
m-Xylene	1.6993	0.7481	1.1741
Naphthalene, 1,2-dihydro-	0.0712	0.0332	1.4032
1H-Indene, 1-ethylidene-	1.7358	2.1059	3.0318
1H-Indene, 2,3-dihydro-4-methyl-	1.4481	1.4824	-

4.1.2.4 Sulfur removal activity

Figure 4.15 shows the weight percentage of sulfur in the pyrolysis oils. The highest sulfur content is found in the non-catalytic case, and can be eliminated by using a catalyst up to ~40 % reduction. HBETA has the greater sulfur removal ability than HY, and the lowest sulfur content is found with using 0.25 % Rh/HBETA, possibly because the hydrogenation of the noble metal could help the saturation of aromatics and double bonds before the aromatic rings are cracked with the release of hydrogen sulfide. On the other hand, Rh has no effect of sulfur reduction when it is loaded on HY. The sulfur distribution in Figure 4.16 assures that the desulfurization of oils has occurred on 0.25 % Rh/HBETA since the sulfur distribution is considerably shifted to the gas range.

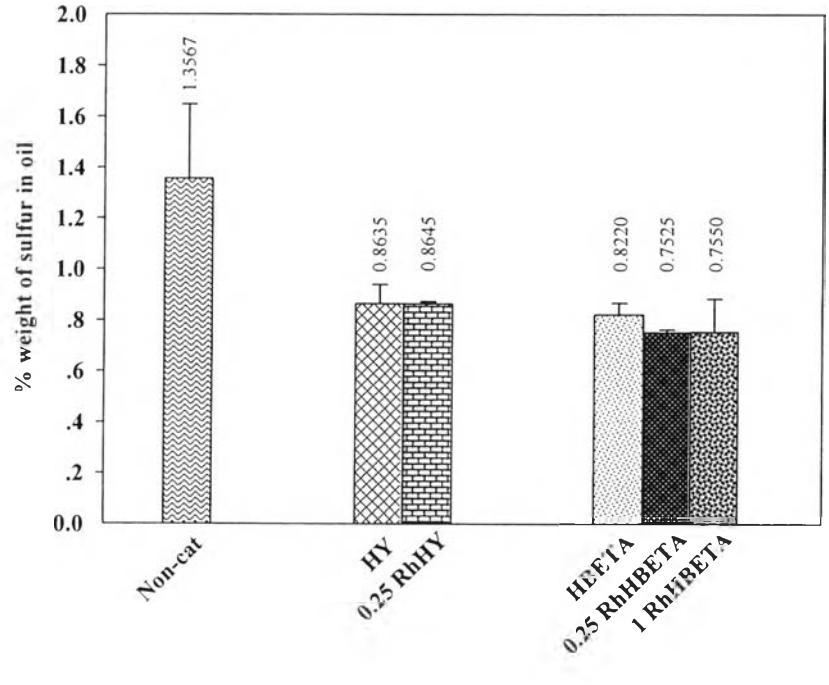

Figure 4.15 % weight of sulfur content in pyrolysis oils obtained from using Rh supported on HY and HBETA.

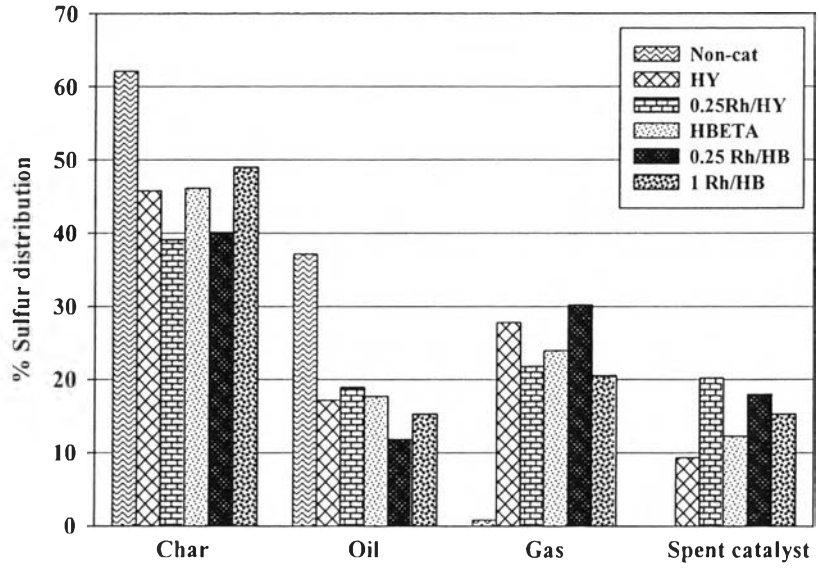

Figure 4.16 Sulfur distribution in pyrolysis products obtained from Rh-promoted HY and HBETA catalysts.

Figure 4.17 shows the distribution of sulfur in light petroleum cuts such as gasoline, kerosene and gas oil fractions. Sulfur is highly distributed in gas oil in the non-catalytic case. Using the catalysts reduces sulfur in the gas oil fraction. The HBETA-supported catalysts results in a high distribution of sulfur in gasoline, especially 0.25 % Rh/HBETA. It can be suggested that the catalysts have the ability in both cracking and desulfurization simultaneously. Table 4.6 shows the prominent C, H, S-containing molecules in each petroleum cuts. It is observed that the sulfur species mostly found in the oils are benzothiophene derivatives.

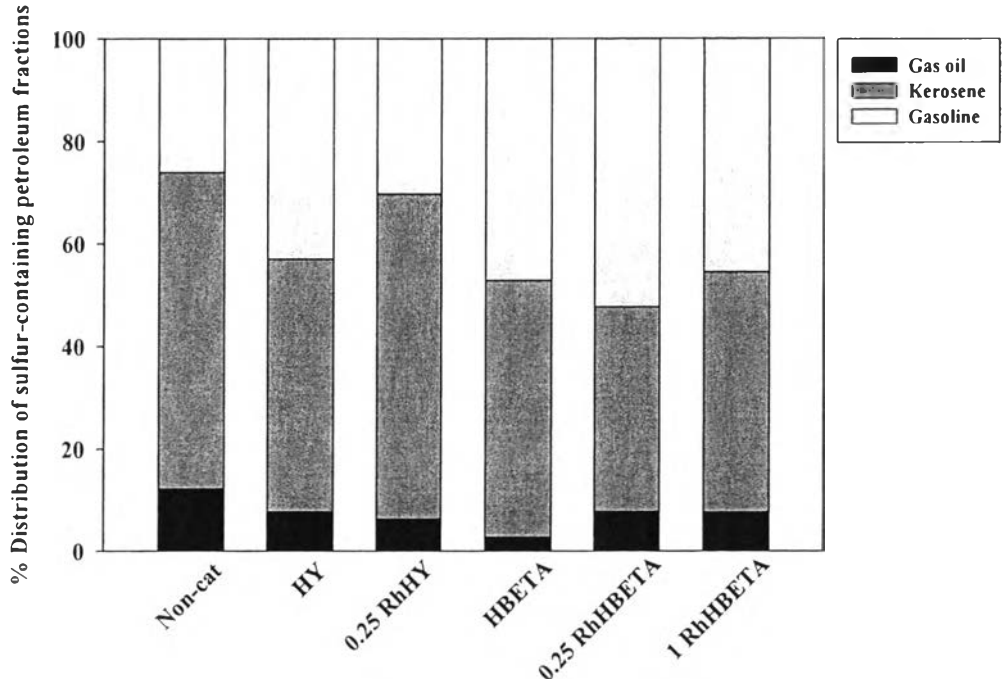

Figure 4.17 Distribution of sulfur-containing compounds in petroleum fractions from Rh supported on HY and HBETA supports.

Table 4.6 Prominent C, H, S-containing molecules found in pyrolysis oils from Rh-promoted HY and HBETA catalysts

Name	Area (%)					
	Non-catalyst	Acidic catalyst				
		HY	0.25Rh HY	HB	0.25Rh HB	1Rh HB
T, 2-(1-methylethyl)-	0.0117	0.0046	0.0115	0.0493	0.0314	0.0189
BT	0.0283	0.0755	0.0621	0.0432	0.0911	0.0888
BT, 2-methyl-	0.0187	0.0114	-	0.0589	0.0005	0.001
BT, 6-methyl-	-	0.0773	-	0.0442	0.0457	0.0458
3-Methyl Benzothiophene	0.0499	0.1043*	0.1382*	0.0247	0.1361*	0.1614*
BT, 2,5-dimethyl-	0.0409	0.1342*	0.0342	0.1068*	0.0249	0.0487
BT, 2,7-dimethyl-	0.1138*	0.0349	0.2153*	0.0316	0.0939	0.1665*
BT, 2-ethyl-7-methyl-	0.0606	0.0892	0.0038	0.0425	0.1001*	0.0025
BT, 2,5,7-trimethyl-	0.0446	0.0057	0.0917	0.0029	0.0056	0.1379*
BT, 7-ethyl-2-methyl-	0.0077	0.0064	0.0552	0.0298	0.0046	0.0055
BT, 2,7-diethyl-	0.0463	0.013	0.0213	0.0556	0.0033	0.0042

T = Thiophene

BT = Benzo[b]thiophene

* The area percentage of C,H,S-containing molecules in maltene fraction greater than 0.1 %

4.2 Commercial hydrodesulfurization catalysts as a tire pyrolysis catalyst

The hydrodesulfurization catalysts, $NiMoS/Al_2O_3$ and $CoMoS/Al_2O_3$, have been used in the petroleum industry for reducing sulfur compounds in the heavy oils under the severe conditions. They have mainly desulfurization activity with a low cracking ability achived from the acid support. Therefore, the commercial sulfided $NiMoS/Al_2O_3$ and $CoMoS/Al_2O_3$ catalysts were examined for their activity on the pyrolysis of waste tire. The effects of the catalysts on pyrolysis products and sulfur reduction are described below.

4.2.1 Regenerated $NiMoS/Al_2O_3$ catalyst

A regenerated commercial sulfided $NiMoS/Al_2O_3$ catalyst from the hydrodesulfurization unit of a refinery in Thailand was employed for waste tire pyrolysis. The regenerated NiMoS alumina catalyst has the potential to be a catalyst for the catalytic pyrolysis of waste tire because it contains both sulfide and acid functions for cracking and removal of sulfur species. Moreover, since it is a spent catalyst, its cost is low, making waste tire pyrolysis more commercially viable. The results of using a regenerated $NiMoS/Al_2O_3$ catalyst are shown as the follows.

4.2.1.1 Pyrolysis yields

The yields of gas, liquid, solid and coke products after the pyrolysis of waste tire with and without the spent commercial sulfided $NiMoS/Al_2O_3$ catalyst are given in Figure 4.18. The results show that spent $NiMoS/Al_2O_3$ decreases the yield of liquid products from ~42 wt% to ~32 wt% by increasing amount of gas products and coke formation while the solid yields gave a bit lower than the non-catalytic case. It means that using the catalyst promotes the decomposition of tire molecules, resulting in a higher amount of lighter molecules than thermal cracking; therefore, high activity is obtained from the catalytic case. It is not surprised that coke is formed on the used catalyst. The amount of coke per gram of the catalyst is shown in Table 4.18.

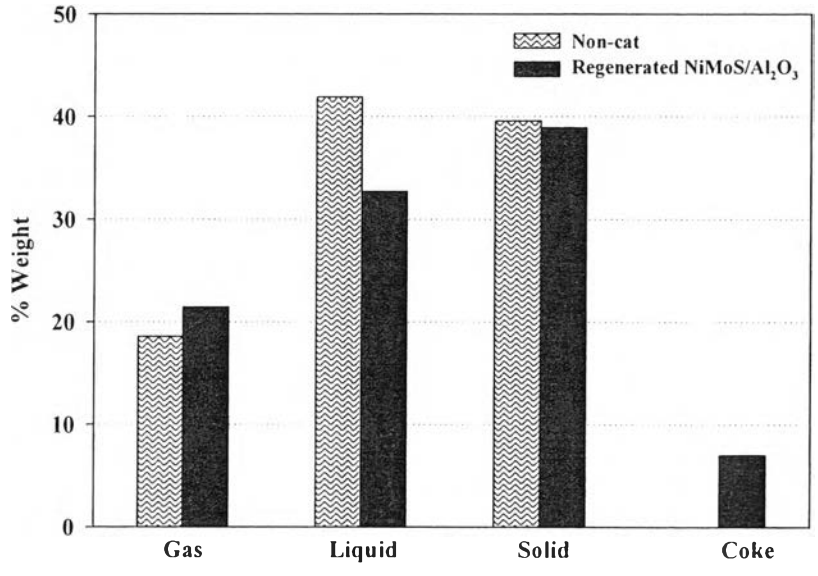

Figure 4.18 Effect of regenerated $NiMoS/Al_2O_3$ on pyrolysis products.

4.2.1.2 Gas composition

Figure 4.19 displays the amount of light gas products acquired from the pyrolysis of waste tire from the catalytic and non-catalytic cases. It is interesting that using the regenerated $NiMoS/Al_2O_3$ shows high selectivity to alkane products, possibly because of the hydrogenation ability (Li-hua *et al.*, 2011, Rodríguez-Castellón *et al.*, 2008 and Kim *et al.*, 2003). It is known that an alkane is a saturated hydrocarbon, so it is easily formed by the hydrogenation. Hence, the regenerated $NiMoS/Al_2O_3$ is a good catalyst for producing light alkane gas products from waste tire pyrolysis as compared to the non-catalytic experiment.

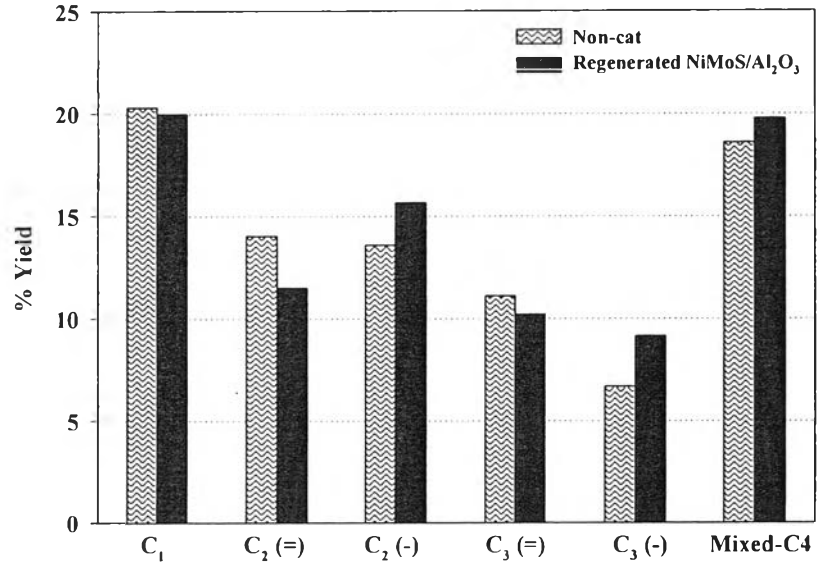

Figure 4.19 Effect of regenerated $NiMoS/Al_2O_3$ on light gas yield.

4.2.1.3 Liquid composition and petroleum cuts

Figure 4.20 shows the chemical composition in the maltenes. It is seen that the regenerated $NiMoS/Al_2O_3$ catalyst can reduce the polar-aromatics, but it gives a low performance in poly-aromatics reduction consequently causing the shortage of the saturated hydrocarbons. The remarkable result of mono-aromatics is found in the catalytic case. The petroleum fractions in maltenes are shown in Figure 4.21. The results indicate that full range naphtha increases in the expense of heavy fractions using the $NiMoS/Al_2O_3$ catalyst. Nevertheless, the minor decrease of long residue is observed due to the mild acidity of Al_2O_3 support.

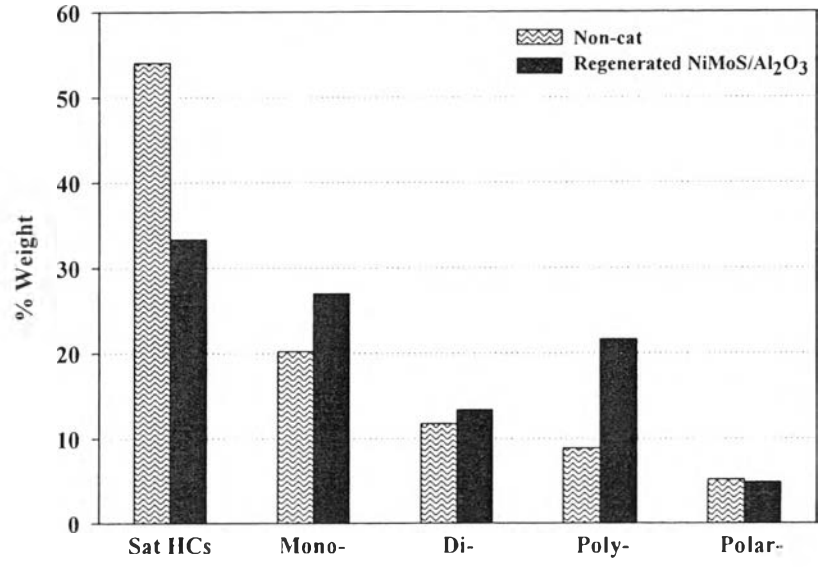

Figure 4.20 Chemical compositions of maltenes obtained from using regenerated $NiMoS/Al_2O_3$.

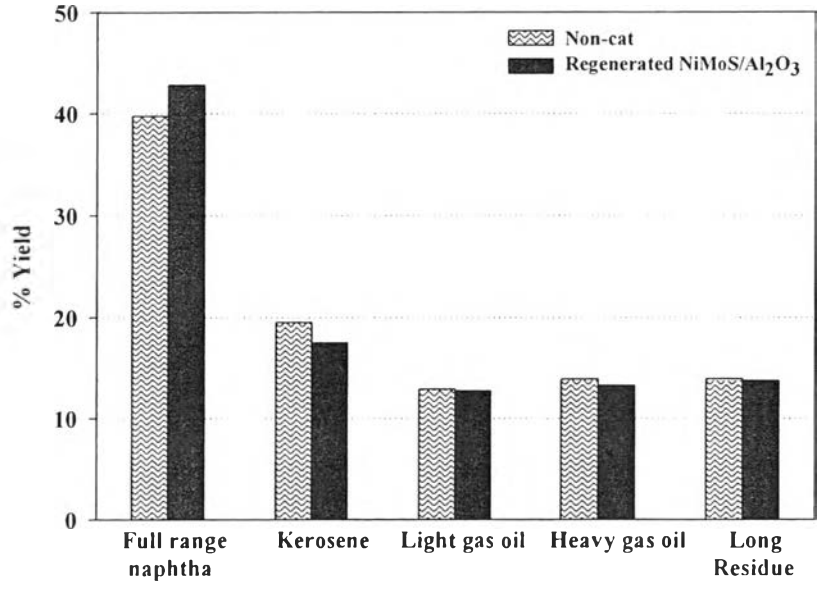

Figure 4.21 Petroleum fractions in derived oils obtained from using regenerated $NiMoS/Al_2O_3$.

According to the results, the shift of all pyrolysis products from using the regenerated $NiMoS/Al_2O_3$ catalyst can be explained by using IPA-TPD results. The TPD profiles in Figure 4.22 present the MS signals of isopropylamine (m/e = 44), ammonia (m/e =17) and propylene (m/e = 41) from a mass spectrometer. The maximum desorption of unreacted isopropylamine is observed at 120 °C, associated to weak acid sites on the surface of the spent $NiMoS/Al_2O_3$ catalyst while the maximum desorptions of propylene and ammonia around 300-400 °C represent Brønsted acid sites due to the fact that isopropylamine is decomposed on Brønsted acid sites (not Lewis acid sites), producing propylene and ammonia. The catalyst has both weak and Brønsted acid sites; however, weak acid sites are dominant, meaning that the catalyst has mild acidity or less amount of strong Brønsted acid sites. It can be explained that the slight changes on heavy to light products are caused by the mild cracking ability of the spent $NiMoS/Al_2O_3$ acid catalyst.

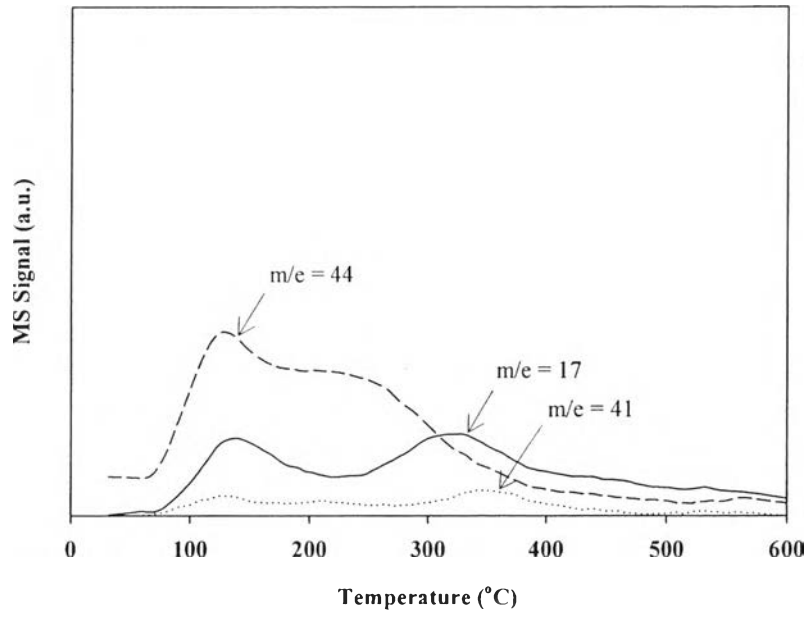

Figure 4.22 IPA-TPD profiles of isopropylamine (m/e = 44) desorption, ammonia (m/e =17) formation, and propylene (m/e = 41) formation on the regenerated $NiMoS/Al_2O_3$ catalyst.

The regenerated $NiMoS/Al_2O_3$ obtained from refinery is analyzed for the elemental composition by using XRF. The concentration of Co, Ni, Mo, S, Si and Al elements are given in Table 4.7. Its specific surface area, pore specific volume and median pore width are reported with amount coke deposited on the used catalyst. It was reported that the γ-Al_2O_3 catalyst caused the deactivation by the major cause of acid sites and coke deposition on the metal particles (Fung *et al.*, 2001). It is possible that the reactions occur mostly in the pore of catalyst, so it can be suggested that coke is formed in the pore of acid catalyst.

Table 4.7 Physical properties of spent $NiMoS/Al_2O_3$ catalyst and the amount of coke in the used catalysts

Sample		**$NiMoS/Al_2O_3$**
Composition (%)	Co	0.017
	Ni	5.994
	Mo	17.20
	S	0.816
	Si	1.061
	Al	74.91
Specific surface area (m^2/g)		198.7
Pore specific volume (cm^3/g)		0.422
Median pore width (Å)		8.855
Coke (g/g cat)		0.356

4.2.1.4 Sulfur removal activity

The sulfur contents in pyrolysis oils obtained from the elemental analyzer are given in Figure 4.23. A high content of sulfur is found in the non-catalytic case; however, it can be reduced from 1.36 to 0.60 wt% by using the catalyst. The disappearance of the sulfur in oil occurs in conjunction with a higher distribution of sulfur in the gas product and the used catalyst as indicated by the sulfur balance (Figure 4.24). The high amount of sulfur in the gas fraction is possibly in the form of H_2S (Lin et al., 1997). It has been reported that H_2S can be adsorbed

on the active site catalyst (Sidhpuria et al., 2008), resulting in a high deposition of sulfur on the spent catalyst. By using the GC-MS (TOF), the distribution of sulfur in light petroleum cuts illustrated in Figure 4.25 indicates that the spent $NiMoS/Al_2O_3$ catalyst can change the high distribution of sulfur, which is formerly in kerosene (C_{10}-C_{13}) and gas oil (C_{14}-C_{20}), to in gasoline (C_5-C_9). It can be concluded that the catalyst has the ability in both cracking and desulfurization simultaneously.

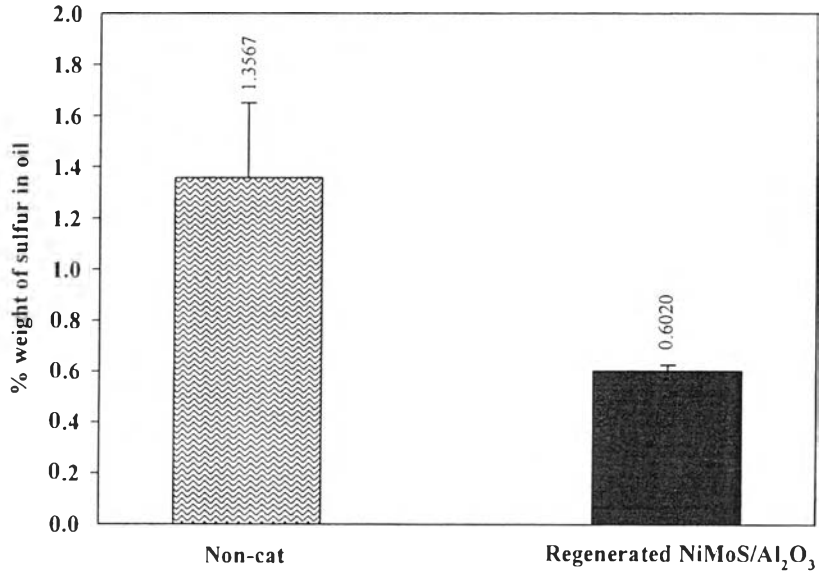

Figure 4.23 Sulfur content in pyrolysis oils obtained from using regenerated $NiMoS/Al_2O_3$.

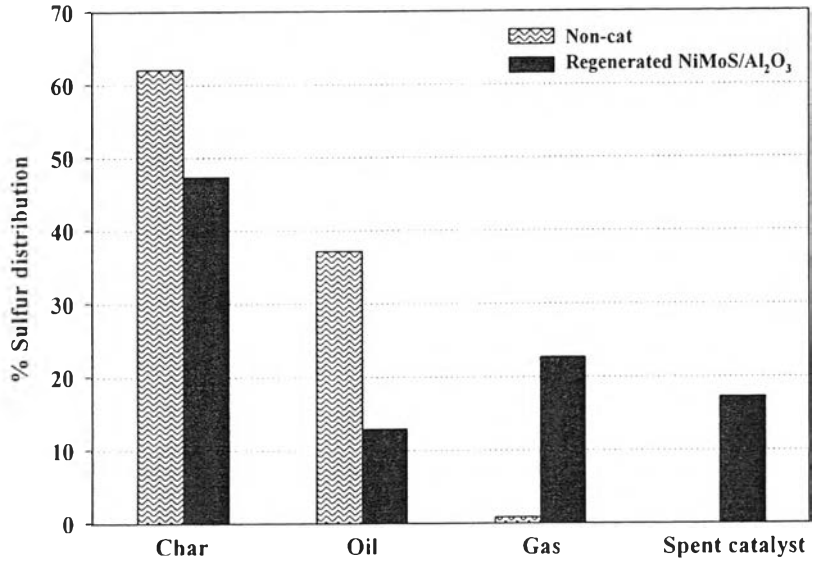

Figure 4.24 Sulfur distribution in pyrolysis products obtained from the regenerated $NiMoS/Al_2O_3$.

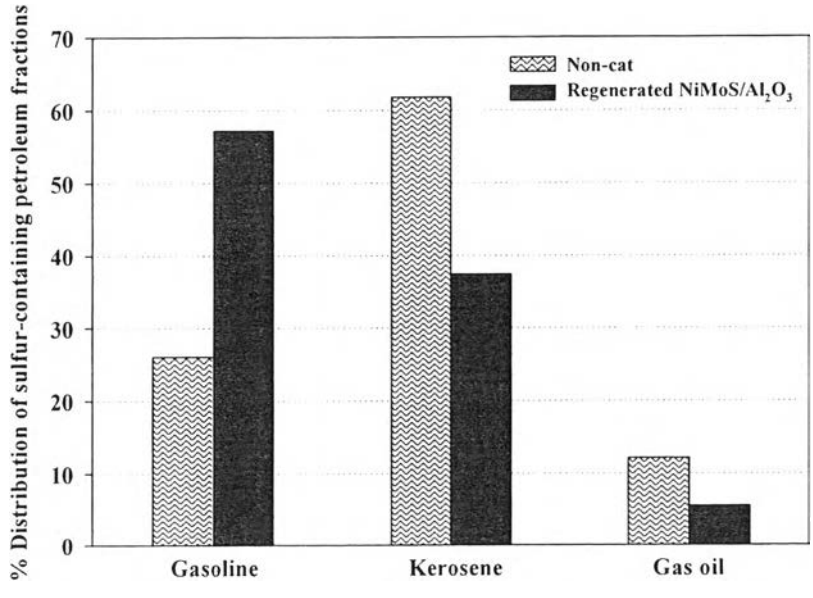

Figure 4.25 Distribution of sulfur in petroleum fractions from using regenerated $NiMoS/Al_2O_3$.

Table 4.8 shows the prominent C, H, S-containing molecules in each petroleum cuts. It is observed that sulfur species obtained in the highest amount from the non-catalytic case are benzo[b]thiophene, 2,7-dimethyl- in kerosene (C_{10}-C_{13}) fraction whereas those observed from the regenerated NiMoS/Al_2O_3 case is 3-methylbenzothiophene in gasoline fraction (C_5-C_9), which contains less number of alkyl groups than the non-catalytic case as shown in Figure 4.8. Most of the sulfur-containing molecules found in gasoline, kerosene and gas oil ranges are benzothiophene derivatives such as 3-methybenzothiophene (C_9H_8S), benzo[b]thiophene, 2,5-dimethyl- ($C_{10}H_{10}S$), and dibenzothiophene derivatives such as naphtho[2,3-b]thiophene, 4,9-dimethyl- ($C_{14}H_{12}S$). However, the sulfur species found the most in this study are benzothiophene derivatives, which is different from Williams and Bottrill (1995) who found dibenzothiophene derivatives in majority.

Table 4.8 Prominent C, H, S-containing molecules found in pyrolysis oils from using the regenerated NiMoS/Al_2O_3

Petroleum cuts	Compounds	Formula	Area (%)*	
			Non-cat.	NiMoS /Al_2O_3
Gasoline	Thiophene, 2-ethyl-5-methyl-	$C_7H_{10}S$	-	0.0523
	Thiophene, 3-(1,1-dimethylethyl)-	$C_8H_{12}S$	-	0.0470
	Benzo[b]thiophene	C_8H_6S	0.0283	0.0613
	3-Methylbenzothiophene	C_9H_8S	0.0499	0.1657
Kerosene	Benzo[b]thiophene, 2,7-dimethyl-	$C_{10}H_{10}S$	0.1138	0.0279
	5-Ethylbenzo[b]thiophene	$C_{10}H_{10}S$	0.0137	0.0529
	Benzo[b]thiophene, 2,5-dimethyl-	$C_{10}H_{10}S$	0.0409	0.0897
	Benzo[b]thiophene, 7-ethyl-2-methyl-	$C_{11}H_{12}S$	0.0077	0.0547
Gas oil	2,8-Dimethyldibenzo(b,d)thiophene	$C_{14}H_{12}S$	0.0062	0.0059
	3,7-Dimethyldibenzothiophene	$C_{14}H_{12}S$	0.0091	0.0067
	Naphtho[2,3-b]thiophene, 4,9-dimethyl-	$C_{14}H_{12}S$	-	0.0140

* % Area of C,H,S-containing molecules in maltene fraction determined by GC-MS (TOF)

4.2.2 Fresh $CoMoS/Al_2O_3$ catalyst

A commercial $CoMoS/Al_2O_3$ hydrodesulfurization catalyst obtained from the refinery in Thailand was used as a catalyst for the pyrolysis of waste tire because it has acid and metal sulfide functions (Al_2O_3 and CoMoS, respectively) that can promote cracking and sulfur reduction simultaneously. The results of using a fresh $CoMoS/Al_2O_3$ catalyst are explained as the following;

4.2.2.1 Pyrolysis yields

The pyrolysis product distributions obtained from with and without the $CoMoS/Al_2O_3$ catalyst are shown in Figure 4.26. Due to the fact that the catalyst promoted the reaction activity, it results in a higher amount of gas and coke formation by the reduction of liquid product. The amount of solid products is quite constant assuring the complete decomposition of tire.

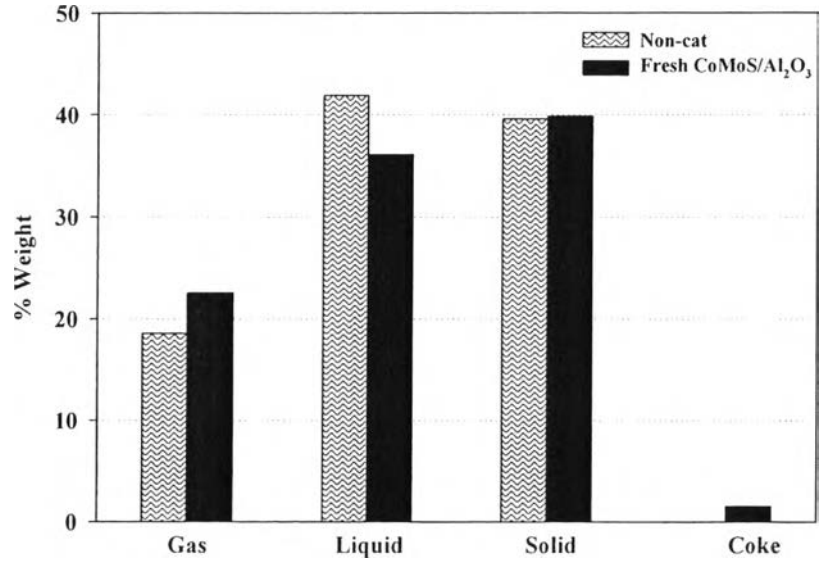

Figure 4.26 Effect of fresh $CoMoS/Al_2O_3$ on pyrolysis products.

4.2.2.2 Gas composition

The amount of light gas products from using $CoMoS/Al_2O_3$ compared with non-catalytic case is shown in Figure 4.27. It is clearly seen that $CoMoS/Al_2O_3$ results in high selectivity of alkane gas product by the reduction of the alkene gas (ethylene and propylene), possibly due to the hydrogenation ability of the Co-Mo catalyst (Villarroel *et al.*, 2008) producing the saturated hydrocarbons.

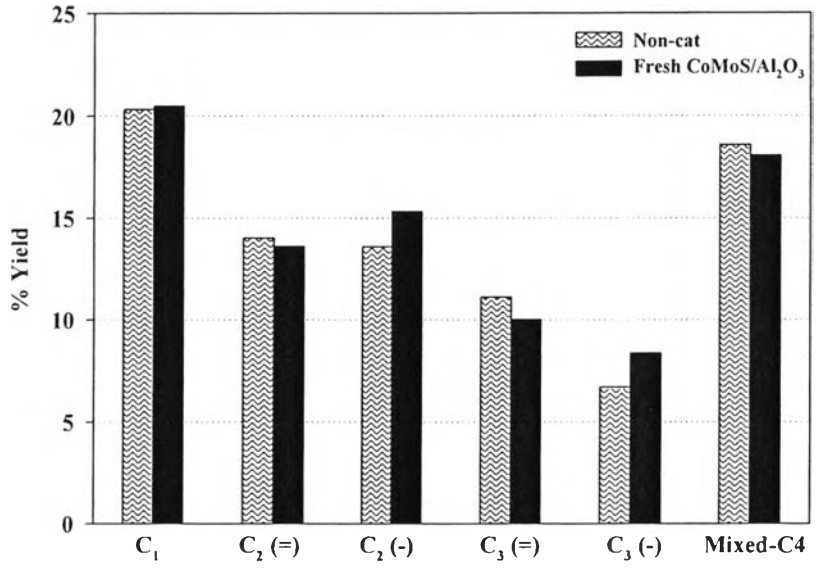

Figure 4.27 Effect of fresh $CoMoS/Al_2O_3$ on light gas yield.

4.2.2.3 Liquid composition and petroleum cuts

The liquid compositions of maltenes obtained from the case of $CoMoS/Al_2O_3$ catalyst were shown in Figure 4.28. It is observed that high amount of mono-aromatics is found in the catalytic case. A commercial $CoMoS/Al_2O_3$ has ability in preventing the polar-aromatics formation, but it has low cracking activity as seen in high amount of remaining poly-aromatics. Figure 4.29 displays the petroleum fractions in the pyrolysis oils. A bit decrease of long residue is found in accordance with the increase in kerosene and gas oil in the catalytic case. The increment of short-chain hydrocarbons (full range naphtha) is not observed owing to the mild acidity of Al_2O_3 support.

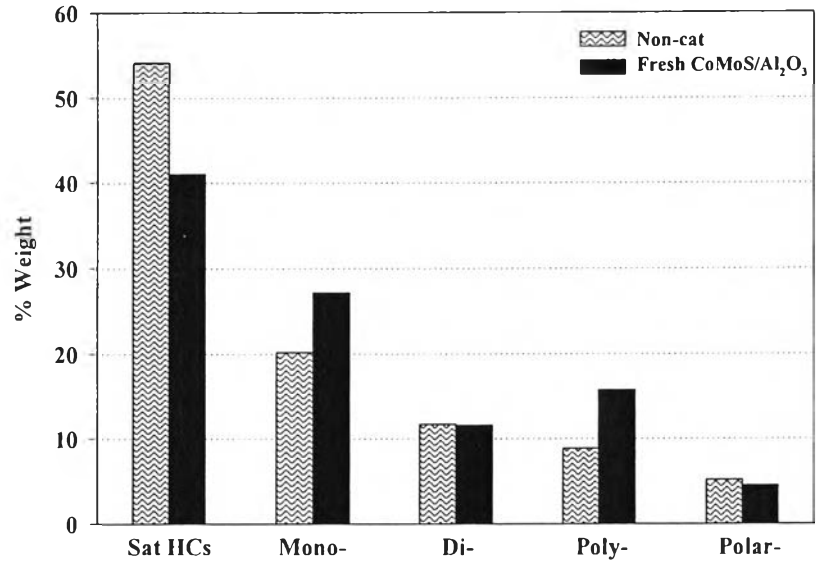

Figure 4.28 Chemical compositions of maltenes obtained using fresh $CoMoS/Al_2O_3$ catalyst.

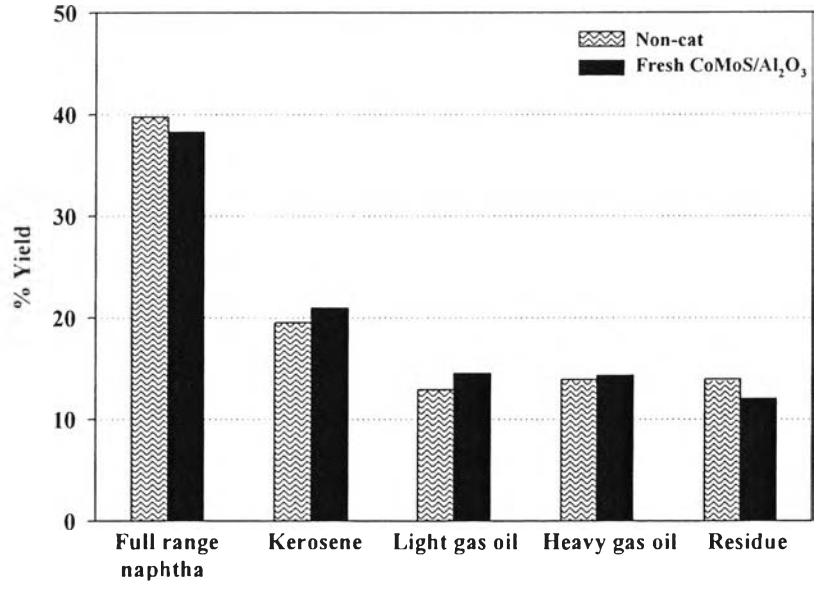

Figure 4.29 Petroleum fractions of derived oils obtained from fresh $CoMoS/Al_2O_3$.

The shift of pyrolysis products could be explained by the acidity of the catalyst that confirmed by elucidating the results obtained from IPA-TPD analysis as shown in Figure 4.30. This figure presents the TPD profiles of isopropylamine (m/e = 44), ammonia (m/e =17) and propylene (m/e = 41) using the $CoMoS/Al_2O_3$ catalyst. Unreacted isopropylamine desorbed from the samples with a maximum desorption at about 120 ^{o}C. The desorption of unreacted isopropylamine can be attributed to weak acid sites on the surface of the $CoMoS/Al_2O_3$ catalyst. The formation of propylene and ammonia were observed at higher temperatures. The presence of propylene and ammonia can assure that the $CoMoS/Al_2O_3$ catalyst has the Brønsted acid sites because of the fact that isopropylamine is decomposed over Brønsted acid sites to propylene and ammonia whose signals can be seen in Figure 4.30. It indicates that the increase in gaseous products in conjunction with the reductions of liquid product and the heavy fractions are caused by the cracking ability of the commercial $CoMoS/Al_2O_3$ acid catalyst. This induces the formation of coke during the cracking reaction. The physical properties of catalyst and the amount of coke in the used catalyst are shown in Table 4.9.

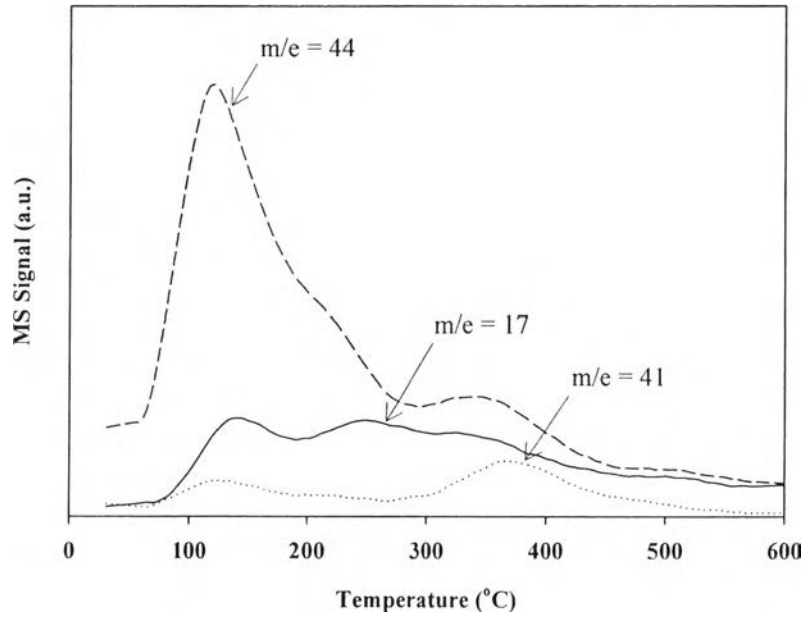

Figure 4.30 IPA-TPD profiles of isopropylamine (m/e = 44) desorption, ammonia (m/e =17) formation, and propylene (m/e = 41) formation on the fresh $CoMoS/Al_2O_3$ catalyst.

Table 4.9 Physical properties of fresh $CoMoS/Al_2O_3$ catalyst and the amount of coke in the used catalyst

Sample		**$CoMoS/Al_2O_3$**
Composition (%)	Co	6.372
	Ni	0.080
	Mo	23.63
	S	1.139
	Si	0.795
	Al	67.98
Specific surface area (m^2/g)		213.9
Pore specific volume (cm^3/g)		0.434
Median pore width (Å)		8.107
Coke (g/g cat)		0.314

4.2.2.4 Sulfur removal activity

The sulfur contents in pyrolysis oil from using $CoMoS/Al_2O_3$ as a catalyst are shown in Figure 4.31. The high concentration of sulfur is observed in the non-catalytic case. The introduction of $CoMoS/Al_2O_3$ catalyst decreases the amount of sulfur from 1.36 to 0.55 wt% in pyrolysis oil. The sulfur distribution in the products in Figure 4.32 indicates that using $CoMoS/Al_2O_3$ catalyst apparently shifts the sulfur in char and oil into the gas product possibly in the form of H_2S gas (Lin *et al.*, 1997) that can poison the catalyst (Sidhpuria *et al.*, 2008), causing a high deposition of S on the spent catalyst. Figure 4.33 exhibits the distribution of sulfur in light petroleum cuts. For the non-catalytic process, the sulfur compounds in light petroleum cuts were distributed the most in kerosene (C_{10}-C_{13}), followed by gasoline (C_5-C_9). The $CoMoS/Al_2O_3$ catalyst shifts sulfur distribution in gas oil and kerosene to gasoline range indicating that the catalyst had the ability in both cracking and desulfurization.

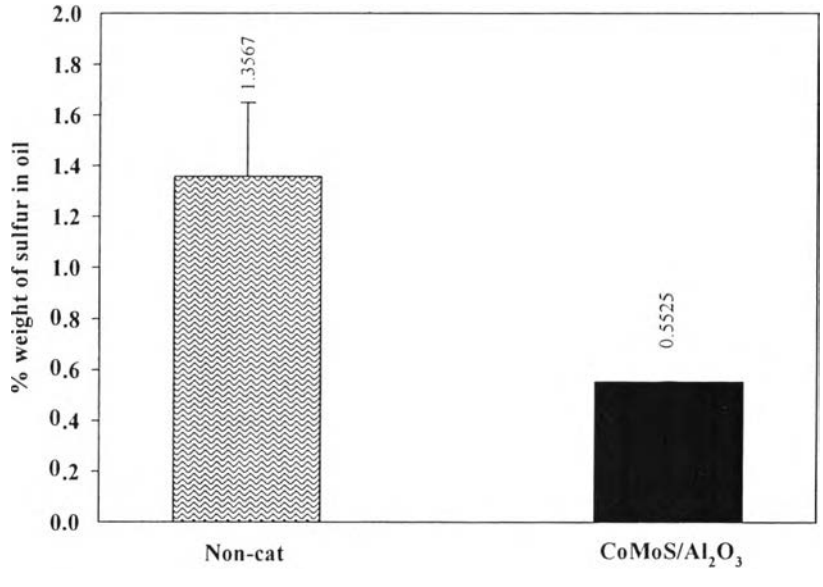

Figure 4.31 Sulfur content in pyrolysis oils obtained from using fresh $CoMoS/Al_2O_3$.

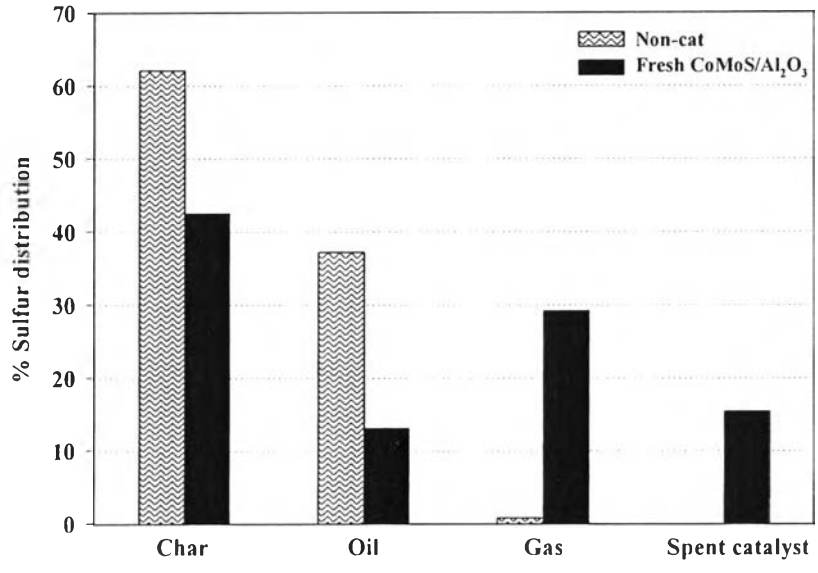

Figure 4.32 Sulfur distribution in pyrolysis products obtained from the experiment of fresh $CoMoS/Al_2O_3$.

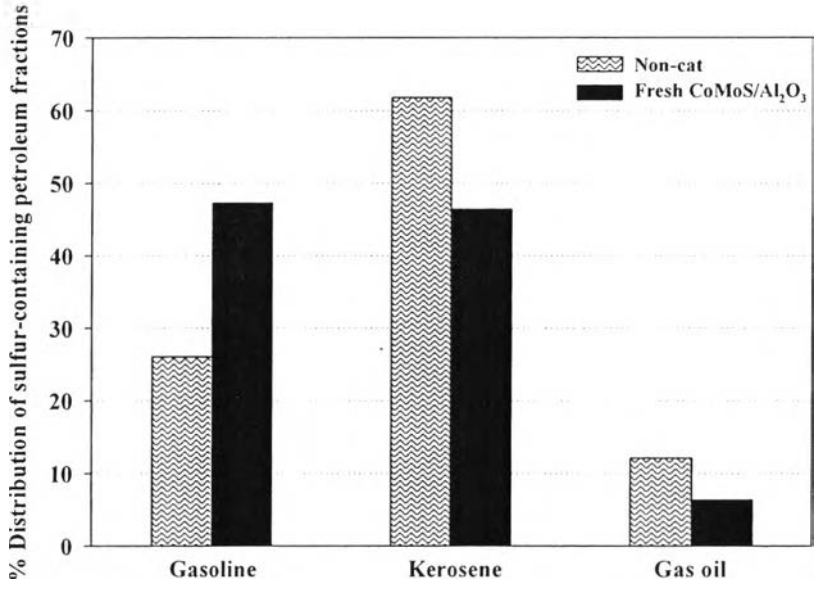

Figure 4.33 Distribution of sulfur in petroleum fractions from using fresh $CoMoS/Al_2O_3$.

The prominent C, H, S-containing molecules in each petroleum cuts of the catalytic case are listed in the Table 4.10. The highest quantity of sulfur species is benzo[b]thiophene, 2,7-dimethyl- in the kerosene fraction. The amount of same sulfur compounds in the non-catalytic case is also reported to compare with the catalytic case. However, the sulfur species mostly found in the experiment of $CoMoS/Al_2O_3$ are benzothiophene derivatives.

Table 4.10 Prominent C, H, S-containing molecules found in pyrolysis oils from using fresh $CoMoS/Al_2O_3$

Petroleum cuts	**Compounds**	**Formula**	**Area (%) [a]**	
			Non-cat.	**CoMoS /Al_2O_3**
Gasoline	Thiophene, 2-(1-methylethyl)-	$C_7H_{10}S$	0.0117	0.0695
	Benzo[b]thiophene	C_8H_6S	0.0283	0.048
	3-Methylbenzothiophen	C_9H_8S	0.0499	0.0913
Kerosene	Benzo[b]thiophene, 2,5-dimethyl-	$C_{10}H_{10}S$	0.0409	0.0401
	Benzo[b]thiophene, 2,7-dimethyl-	$C_{10}H_{10}S$	0.1138	0.1452
	Benzo[b]thiophene, 7-ethyl-2-methyl-	$C_{11}H_{12}S$	0.0077	0.0509
	Benzo[b]thiophene, 2,5,7-trimethyl-	$C_{11}H_{12}S$	0.0446	0.0474
Gas oil	1,7-Dimethyldibenzothiophene	$C_{14}H_{12}S$	0.0145	0.0133
	2,7-Dimethyldibenzothiophene	$C_{14}H_{12}S$	0.0222	0.0081
	2,8-Dimethyldibenzo(b,d)thiophene	$C_{14}H_{12}S$	0.0062	0.0068

* % Area of C,H,S-containing molecules in maltene fraction determined by GC-MS (TOF)